Published in final edited form as:
*Biomaterials*. 2011 December ; 32(34): 8783–8796. doi:10.1016/j.biomaterials.2011.08.010.

# Biocompatibility and biofilm inhibition of *N,N*-hexyl,methyl-polyethylenimine bonded to Boston Keratoprosthesis materials

**Irmgard Behlau**[1,2,4,5,*], **Koushik Mukherjee**[3], **Amit Todani**[1], **Ann S. Tisdale**[2], **Fabiano Cade**[1], **Liqiang Wang**[1], **Elizabeth M. Leonard**[6], **Fouad R. Zakka**[1], **Michael S. Gilmore**[1,5], **Frederick A. Jakobiec**[1,5], **Claes H. Dohlman**[1,5], and **Alexander M. Klibanov**[3]

[1]Ophthalmology, Massachusetts Eye and Ear Infirmary, Boston, MA 02114

[2]Schepens Eye Research Institute, Boston, MA 02114

[3]Departments of Chemistry and Biological Engineering, Massachusetts Institute of Technology, Cambridge, MA 02139

[4]Division of Infectious Diseases, Department of Medicine, Mount Auburn Hospital, Cambridge, MA 02138

[5]Harvard Medical School, Boston, MA 02115

[6]Henry Whittier Porter Bacteriology Laboratory, Massachusetts Eye and Ear Infirmary, Boston, MA 02114

## Abstract

The biocompatibility and antibacterial properties of *N,N*-hexyl,methyl-polyethylenimine (HMPEI) covalently attached to the Boston Keratoprosthesis (B-KPro) materials was evaluated. By means of confocal and electron microscopies, we observed that HMPEI-derivatized materials exert an inhibitory effect on biofilm formation by *Staphylococcus aureus* clinical isolates, as compared to the parent poly(methyl methacrylate) (PMMA) and titanium. There was no additional corneal epithelial cell cytotoxicity of HMPEI-coated PMMA compared to that of control PMMA in tissue cultures *in vitro*. Likewise, no toxicity or adverse reactivity was detected with HMPEI-derivatized PMMA or titanium compared to those of the control materials after intrastromal or anterior chamber implantation in rabbits *in vivo*.

### Keywords

antibacterial; polyethylenimine (PEI); keratoprosthesis; PMMA; titanium; *Staphylococcus aureus*; corneal cytotoxicity

## 1. Introduction

Indwelling prosthetic devices have been critical in saving numerous lives and they have enhanced the quality of life for even more patients [1]. Yet the presence of an indwelling foreign body both predisposes to, and complicates the eradication of, infections, often with



*Corresponding author: irmgard_behlau@meei.harvard.edu; Fax: 1-617-573-4369.

biofilm formation [2]. Device-related biofilm infections account for some 60% of all hospital-associated infections [3] and add about $5 billion per year to U.S. hospital costs [4]. Biofilms, heterogenous collections of bacteria often encased by a secreted matrix called extracellular polymeric substance (EPS) [5], adhere strongly to surfaces, are resistant to antibiotics and other biocides, and are protected from host immune defenses [6]. The risk of a biofilm-associated medical device infection depends on its location, with any implantable device that translocates from the surface of the body (skin, cornea) into a sterile body site (blood, urine, intraocular) being at greater risk [2,7].

The Boston Keratoprosthesis (B-KPro) is an artificial cornea that is a treatment option for corneal disorders not amenable to standard penetrating keratoplasty (corneal transplantation) [8]. The B-KPro has the shape of a collar button and consists of a transparent medical-grade poly(methyl methylacrylate) (PMMA) front plate with a stem, that houses the optical portion of the device, and a back plate with holes composed of either PMMA or medical-grade titanium. During implantation, the device is assembled with a donor corneal graft positioned between the front and back plates with extension of the optic stem into the anterior chamber of the eye; a titanium C-ring locks the assembly (Figs. 1A to 1C) [9]. Its postoperative management includes the continuous wearing of a soft contact lens to prevent ocular surface dehydration and tissue melt [10]. Daily low-dose topical antibiotic prophylaxis is required [11], as well as low-dose topical steroids in many patients [9]. While the use of life-long daily antibiotic prophylaxis to prevent infection has been effective, long-term medication adherence and emergence of resistant organisms continue to be concerns, especially in the developing world [12].

Thus there is a great need for keratoprostheses and other implantable medical devices that inherently resist bacterial infection long-term. Most biocidal products depend on a timed release of antibiotics, heavy metal ions (notably silver), or other biocides. Once all biocide has been released, the antimicrobial activity ends, leaving foreign material *in situ*; consequently, the overall long-term benefit of antibiotic-impregnated materials remains unclear [13]. Given the large health care costs of medical-device and hospital-acquired infections [4], non-toxic materials that effectively and permanently limit microbial adherence and viability are very much needed.

It would be most desirable to permanently attach coatings onto PMMA and other currently used prosthetic materials that either prevent adherence of bacteria or kill them on contact, thereby inhibiting the formation of biofilms. Recently, non-leaching, long-chained hydrophobic polycations that can be attached covalently to the materials' surfaces and render them strongly antimicrobial have been developed [14,15]. Specifically, immobilized *N,N*-hexyl,methyl-polyethylenimine (HMPEI) (Fig. 1D) has broad antibacterial, antifungal, and antiviral properties [16-19].

Herein we assess HMPEI covalently attached to PMMA and titanium materials used in the construction of the B-KPro. Antimicrobial efficacy against hyperbiofilm-forming clinical isolates of *Staphylococcus aureus* and *in vitro* cell cytotoxicity using immortalized human corneal epithelial cells were investigated. *In vivo* biocompatibility studies with new ocular models in the rabbit comparing HMPEI-derivatized and parent PMMA and titanium, as well as the B-KPro with applicability to other implantable medical devices, were examined.

## 2. Materials and Methods

### 2.1 Materials

Laboratory chemicals, branched 750-kDa PEI [19], 500-kDa poly(2-ethyl-2-oxazoline), and organic solvents were from Sigma-Aldrich Chemical Co. (St. Louis, MO). Linear PEI (217 kDa) was prepared by deacylation of poly(2-ethyl-2-oxazoline) as previously described [19].

The Boston Keratoprosthesis (B-KPro) parent materials were medical-grade poly(methyl methacrylate) (PMMA) (Spartech Townsend, Pleasant Hill, IA) and titanium (Ti) 6-4 ELI (Dynamet, Washington, PA) processed by J.G. Machine Co (Woburn, MA). PMMA discs were cut from a 1 cm rotating PMMA rod in 200- and 150-micron thickness. Smaller PMMA discs (3, 1.5, and 1.0 mm) were punched out using Micro Punch Set (Micro-Mark, www.micromark.com). Titanium discs (10, 3.0, and 1.0 mm in diameter) were punched from a single Ti sheet (150 micron in thickness). KPro front pieces (KPro-FP) were made of either a large (KPro-FP-L) 4.75 mm front plate diameter and 3.3 mm stem diameter or a smaller (KPro-FP-S) 2.7 mm front plate diameter and 1.5 mm stem diameter; all had a 2 mm stem length. B-KPro Type I threaded design (pseudophakic) had a front plate diameter of 5.0 mm and a stem diameter of 3.35 mm. The PMMA threaded back plate had a diameter of 8.5 mm, plate thickness of 0.8 mm, and 16 holes of 1.2 mm in diameter each. The daily wear contact lens was composed of nelfilcon A (Focus Dailies™, diameter of 13.8 mm; CIBA Vision Co., Duluth, GA). The bandage contact lens was composed of methafilcon (Kontur Precision Sphere, diameter of 16 mm, base 8.6-9.8; Kontur Kontact Lens, Hercules, CA).

Povidone-iodine ophthalmic solution 5% (Betadine 5%™, Alcon, Fort Worth, TX) was used as a preoperative antiseptic. Polymyxin B (10,000 polymyxin B U/mL and 1 mg trimethoprim sulfate) ophthalmic solution USP with benzalkonium chloride 0.004% preservative (Bausch & Lomb, Tampa, FL) and prednisolone acetate ophthalmic solution 1% (Falcon Pharmaceuticals (Alcon), Fort Worth, TX) were obtained from the Massachusetts Eye and Ear Infirmary (MEEI) Pharmacy. Balanced salts solutions (BSS™ and BSS Plus™, Alcon) were used for ocular irrigation. Xylazine injectable solution 100 mg/mL (Tranquived, Vedco, St. Joseph, MO), ketamine HCl USP 100 mg/mL (Ketaject™, Phoenix Pharm, St. Joseph, MO), and proparacaine HCl ophthalmic solution USP 0.5% (Bausch & Lomb) were used as anesthetic agents. Pentobarbital solution 390 mg/mL (Fatal-Plus, Vortech Pharm, Dearborn, MI) was used for euthanasia.

The surgical dissecting instruments were Super Sharp Blade, 30 degree, 3.5 mm (K-blade, Katena Products, Denville, NJ), crescent microsurgical knife 2.0 mm angled, bevel up blade (Katena Products), Graefe micro dissecting knife, 0.5 mm tip diameter (Fine Science Tools, Vancouver, British Columbia, Canada), trephine 8.5mm (Storz Instruments, Bausch & Lomb), and 3 mm and 1.5 mm biopsy punches (Acu-Punch, Acuderm, Ft. Lauderdale, FL). Black monofilament nylon (Ethilon™ 10-0 and 8-0) and coated polyglactin 910 (Vicryl™ undyed braided 6-0) were used for suturing (Ethicon (Johnson & Johnson), Somerville, NJ).

### 2.2 Strains and Media

Because *Staphylococcus aureus* is a normal commensal on the skin and ocular surface, yet infection (including device-associated biofilm infections [3]) appears to be predominantly caused by a subset of organisms that possess certain microbiologic virulence traits [20-23], we first screened infection-causing *S. aureus* clinical isolates for their ability to form biofilms. Since previous reports have indicated the influence of media composition on *in vitro* biofilm production, we evaluated our clinical isolates for biofilm production under various media and growth conditions (Table 1).

Fourteen *S. aureus* clinical isolates, including methicillin-sensitive and methicillin-resistant ones, were obtained from the MEEI Porter Bacteriology Laboratory [24]. They were frozen within two passages to minimize loss of *in vivo* virulence from representative eye, skin, and mucous membrane infections. Three well-characterized *S. aureus* strains (gift of Dr. G. Pier, Channing Lab, Boston, MA) [25] served as biofilm controls: (i) MN8 [26], a toxic shock syndrome clinical isolate, that produces moderate amount of biofilm (MN8 mucoid, MN8m); (ii) a spontaneous mutant isolated from a chemostat culture of MN8 that constitutively overproduces the polysaccharide intercellular adhesion [poly(*N*-acetyl-1,6-glucosamine)], a hyperbiofilm strain; and (iii) an isogenic mutant, MN8mΔ*ica*(*x02237*)*tet*, containing a deletion in the *ica* locus which impairs biofilm formation. Minimal inhibitory concentrations (MIC) were determined on planktonic bacteria by Clinical Standards and Laboratory Institute methods [27]. Strains were evaluated for biofilm production in three antibiotic-free media (brain heart infusion (BHI), trypticase soy broth (TSB), and Luria-Bertani (LB)), with various carbohydrate sources (glucose and sucrose) and concentrations, and at different time points.

### 2.3 Material Derivatizations

Linear and branched *N,N*-dodecyl,methyl-PEIs (DMPEIs) (from 217-kDa PEI), synthesized as previously described [19], were used only for initial *in vitro* biofilm studies. PMMA discs were painted with DMPEI dissolved in butanol (50 mg/mL) by brush coating both sides three times.

Surface covalent modifications of PMMA and titanium materials, including the B-KPro, for microscopy, cytotoxicity, and all *in vivo* studies employed linear *N,N*-hexyl,methyl-PEI (HMPEI).

Covalent derivatization of PMMA [28] was performed as schematically illustrated below.


In Step 1, PMMA discs were treated with 4 M NaOH at 50°C for 90 min, washed, and incubated in 10% aqueous citric acid overnight. The discs obtained in Step 1 were washed with water until the pH of the washings became neutral, followed by air-drying. In Step 2, the partially surface-hydrolyzed PMMA discs were treated with a 1:1 (v/v) DMF/water solution containing 1.2 g of linear PEI, 4.5 g of 1-hydroxybenzotriazole, and 4.5 g of (3-(dimethylamino)propyl)ethyl-carbodiimide HCl. Following a 18-h incubation at room temperature, the discs were thoroughly washed with water and dried in air. In Step 3, PEI-modified PMMA discs from Step 2 were treated with a 6:6:3.5 (v/v) mixture of 1-bromohexane, triethylamine, and *tert*-amyl alcohol at room temperature for 3 h and then thoroughly washed. In Step 4, they were treated with a 1:1 (v/v) mixture of iodomethane and *tert*-amyl alcohol for 1 h, followed by washing with water and methanol. PMMA back plates and screws were covalently derivatized with *N,N*-hexyl,methyl-PEI in the same manner. To quantify the quaternary ammonium groups on the surface of the derivatized PMMA discs, they were titrated with fluorescein [18]. The typical quaternary ammonium group surface density was in the range from 3.4 to 4.7 nmoles per square centimeter.

Covalent modification of titanium discs [29] was performed as schematically shown below.

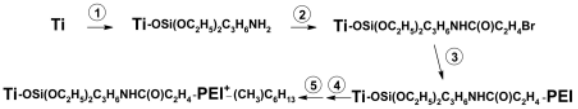

In Step 1, Ti disks were rinsed with toluene and treated at 25°C for 2 h with a 1:1 (v/v) mixture of concentrated $H_2SO_4$ and 30% aqueous $H_2O_2$. The cleaned and oxidized samples were then rinsed with water and dried under vacuum. In Step 2, the surface-oxidized disks were silanized [29] by heating them for 4 h in refluxing toluene containing 10% (3-aminopropyl)triethoxysilane, followed by rinsing with toluene and drying under vacuum. In Step 3, the silanized Ti discs were treated with 4-bromobutyryl chloride in chloroform at room temperature for 5 h and then washed with chloroform to remove any remaining acylating agent. In Step 4, the discs from Step 3 were treated with a solution of 1 g of linear PEI and 90 mg of KOH in 10 mL of *tert*-amyl alcohol at 70°C for 12 h, followed by washing with water and methanol and drying under vacuum. In Step 5, the discs from Step 4 were first treated with a solution of 1.2 mL of 1-bromohexane and 90 mg of KOH in 8 mL of *tert*-amyl alcohol at room temperature, followed by washing with water and methanol and drying under vacuum, and then further alkylated with 1 mL of iodomethane in 4 mL of *tert*-amyl alcohol.

The covalent modification of contact lenses (nelfilcon and methafilcon) was carried out by modifying the hydroxyl groups on the surface with 4-bromobutyryl chloride, followed by the reaction with PEI and alkylation with hexyl bromide and methyl iodide. The modification of the contact lenses needs further optimization in order to minimize drying and refinements will continue.

### 2.4 Cleaning and Sterilization

All materials were washed in a mild detergent with ultrasonic bath cleaning, rinsed thoroughly with distilled water, and ethanol dried. Materials were sterilized by ethylene oxide at 37°C.

### 2.5 Confocal Scanning Light Microscopy

To assess *in vitro S. aureus* biofilm formation and adherence, overnight cultures were grown from a freshly streaked single colony in BHI-2% sucrose, back diluted 100-fold, and aliquoted onto 1-cm sterile discs (HMPEI-PMMA and PMMA; HMPEI-Ti and Ti) in 24-well cell culture dishes for 24 h and 6 days under static growth conditions at 37°C.

Samples were washed with 0.9% NaCl, stained with acridine orange, affixed to a small clear plastic Petri dish, and examined using a Leica TCS-SP2 confocal scanner connected to an inverted microscope (Leica Microsystems, Heidelberg, Germany). For 100X oil-immersion objective, 0.9% NaCl was added to the Petri dish. 3-D confocal images and sequential scans at 488 and 568 nm were obtained. Due to the autofluorescence of HMPEI coated-materials, a third channel, at 633 nm, was added. One-micron sequential scans were obtained from four predetermined representative areas. These experiments were performed in triplicate on separate days.

### 2.6 Field Emission Scanning Electron Microscopy

*In vitro S. aureus* biofilm samples were grown as described in the preceding section. Both *in vitro* and *in vivo* samples were fixed with ½ strength Karnovsky's solution, dehydrated through a graded ethanol series, critical-point dried (Autosamdri 795 Supercritical Point Dryer, Tousimis, Rockville, MD), and mounted and sputter coated with chromium (Model 681 Ion Beam Coater, Gatan, Pleasanton, CA). The entire surface of each specimen was examined with a field emission scanning electron microscope (JEOL 7401F; JEOL, Tokyo, Japan).

### 2.7 *In vitro* Biofilm Analysis of *S. aureus* Isolates

*S. aureus* clinical isolates from MEEI Clinical Laboratory and two laboratory biofilm-positive and biofilm–negative strains were screened for biofilm formation by a static microtiter plate biomass assay using a crystal violet stain [30]. Overnight *S. aureus* cultures were diluted 100-fold in non-selective media with various carbohydrate sources and aliquoted into 96-well polystyrene flat-bottomed microtiter plates at 0.2 mL per well (Corning Life Sciences, Corning, NY). After 24, 48, or 96 h at 37°C, the wells were washed three times with phosphate-buffered saline (PBS) and stained with crystal violet. Eluted crystal violet absorbance at 595 nm was measured by spectrophotometry (Tecan GENios microplate reader, Phoenix Research Products, Research Triangle Park, NC). Experiments were performed in triplicate and repeated three times; the data were then averaged. The mean absorbance value obtained from media control well was deducted from all the test absorbance values. A representative biofilm robustness grading system was assigned to each strain under different growth conditions (Table 1).

### 2.8 Screening Different PEI Variants for *S. aureus* Biofilm Formation Inhibition

DMPEI branched and linear variants [16,19] painted on PMMA were compared using the aforementioned representative robust biofilm-forming ocular isolates and *S. aureus* biofilm laboratory strains. For covalent modifications of HMPEI, only linear PEIs were used. Cultures were grown as above in BHI with 2% sucrose, diluted 100 fold, and 1 mL was aliquoted into 24-well tissue culture plates (Corning Life Sciences) with each well containing a 1-cm disc. Plates were incubated overnight without shaking at 37°C, and biomass was measured by crystal violet staining assay.

### 2.9 *In vitro* Human Corneal Epithelial Cell Cytotoxicity Assays

Telomerase-immortalized human corneal-limbal epithelial (HCLE) cells were obtained from Dr. I. Gipson (Schepens Eye Research Institute, Boston, MA) and plated at $2 \times 10^4$ cells/$cm^2$ in 24-well tissue culture plates (Laboratory-Tek, Naperville, IL) in keratinocyte serum-free medium (K-SFM; Invitrogen-GIBCO, Carlsbad, CA) at 37°C in a 5 % $CO_2$ [31]. After stratification of the corneal cells [31], 1-cm PMMA and HMPEI-PMMA discs were placed on the apical epithelial cells, and cell surface damage was assessed with rose bengal stain [31]. Morphological and cytotoxicity experiments were performed in triplicate on three separate days. Phase contrast morphological assessment was with an inverted light microscope (Eclipse TS100/100-F Nikon, Tokyo, Japan). Micrographs were taken with a digital camera (SPOT Insight Fire Wire; Diagnostic Instruments, Sterling Heights, MI). Quantitative assessment of cell cytotoxicity was performed measuring the cytosolic enzyme lactate dehydrogenase (LDH) released upon lysis of HCLE cells (CytoTox96™, Promega, Madison, WI); absorbances at 490 nm were measured. Experiments were performed in triplicate on three separate days. Statistical analysis used unpaired two-sample equal variance *t*-test (Excel TTEST, MIcrosoft).

### 2.10 Optical Testing

To detect any optical changes to the B-KPro Type I, both uncoated and coated devices were assessed. The B-KPro was clamped in a black iris diaphragm mounted on the rail of an optical bench containing a 3× and 10× objectives. The microscope was moved vis-à-vis the B-KPro until the illuminated Snellen's chart positioned at 20 ft became sharply focused.

### 2.11 *In vivo* Toxicity Studies

All animals used in this study were treated in accordance with the Association for Research in Vision and Ophthalmology (ARVO) Statement for the Use of Animals in Ophthalmic and Vision Research and were approved by the Massachusetts Eye and Ear Infirmary

Institutional Animal Care and Use Committee (Boston, MA). Only one eye per animal was used. The New Zealand white rabbits (Millbrook Farm Breeding Lab, Amherst, MA) weighed between 3.5 and 5.0 kg were anesthetized with intramuscular injection of ketamine HCl (35 mg/kg) and xylazine HCl (10 mg/kg). The BALB/c mice were 20-30 grams in weight (Charles River Laboratories, Wilmington, MA) and received a combination xylazine/ketamine mixture intraperitoneally (50 mg/kg).

Anesthesia was given 15 min prior to surgery. Topical proparacaine HCl 0.5% was instilled into the conjunctival sac of the eye, and the operating area was sterilized with 5% povidine-iodine and repeated after 5 min. Topical ophthalmic antibiotics (Polytrim™) were given immediately pre-operatively. Animals were placed in a laterally recumbent position for surgery.

In clinical assessment, performed by two independent observers, ten parameters were assessed: corneal haze/infiltrate, edema, and neovascularization; conjunctival irritation/chemosis and discharge; epithelial abnormalities; anterior chamber cells and/or flare; iritis +/− pupil size; retroprosthetic membranes; and cataract formation. The first six parameters were evaluated for all clinical examinations, while the last four were also evaluated by slit lamp biomicroscopy. These were graded on a scale from 0 (absent) to 4 (most severe) in relationship to the materials used and potential confounders (surgical wound and sutures) with a theoretical maximum of 40 (Table 2).

Photography was performed using Nikon D90 digital single-lens reflex (SLR) camera attached either to a Zeiss digital SLR camera adapter for the Zeiss OPMI Lumera/S7 ophthalmic surgical microscope (Carl Zeiss Surgical GmbH, Oberkochen, Germany) or directly to Topcon slit lamp microscope (Kogaku Kikai, Tokyo, Japan).

Immediately after euthanasia, animal eyes were enucleated and fixed in neutral buffered formalin, dehydrated, embedded in paraffin, sectioned, and stained with hematoxylin and eosin.

**2.11.1 Intrastromal disc reactivity model—**In BALB/c mice, a cornea incision was made with a Super Sharp blade, and a lamellar corneal micropocket was created using a Graefe microdissecting knife. Either PMMA or HMPEI-PMMA 1- mm discs were placed intrastromally in one eye of each animal. The corneal wound was closed with one 10-0 nylon suture in the earlier pilot experiments. In subsequent experiments, the corneal wound was left unsutured. A partial tarsorrhaphy with one 8-0 suture was performed on all animals. One dose of antibiotics pre-operatively and immediately postoperatively was given. No post-operative antibiotics or topical steroids were administered. (n = 4 groups)

In the New Zealand white rabbit, a cornea incision in the periphery of the cornea was made with a Super Sharp blade. A lamellar corneal micropocket was tunneled to the corneal center using a 2.0-mm angled, bevel-up crescent microsurgical knife. Comparative parent PMMA or HMPEI-PMMA discs (3.0 and 1.5 mm in diameter) and of parent Ti or HMPEI-Ti discs (6-4 ELI; 3.0 mm in diameter) were placed intrastromally in one eye of each animal. The corneal wound was closed with two 10-0 nylon sutures in the earlier pilot experiments; subsequently, it was left unsutured with lengthening of the corneal tunnel pocket. A partial tarsorrhaphy with three 6-0 sutures was performed on all animals and removed by the third day. One dose of polymyxin B/trimethoprim pre-operatively, immediately postoperatively, and daily for two subsequent postoperative days was given; no steroids were given (3-mm discs, n = 4 groups; 1.5-mm discs, n = 3 groups).

**2.11.2 Anterior chamber disc reactivity model in the rabbit—**A corneal incision was made through the cornea into the anterior chamber using a Super Sharp blade. PMMA and HMPEI-PMMA discs, 3 mm in diameter, were placed into the anterior chamber. The corneal wound was closed with two 10-0 nylon sutures and removed within one week. Immediately post-operatively and daily for two subsequent days, topical antibiotic polymyxin B/trimethoprim ophthalmic solution and a topical steroid, prednisolone acetate 1% ophthalmic suspension, were given. (n = 1 set)

**2.11.3 Keratoprosthesis front piece intrastromal-anterior chamber reactivity model in the rabbit—**To assess reactivity in the two major eye compartments that the B-KPro resides in (corneal stroma and anterior chamber) and to enable evaluation in the anterior chamber without floating or uncontrolled attachment to adjacent tissues, we developed a two-compartment eye model using differently sized B-KPro front pieces, B-KPro-FP-L (4.75-mm front plate/3.3-mm stem diameter) and B-KPro-FP-S (2.7-mm front plate/1.5-mm stem diameter). The rabbit cornea was dissected vertically to 50% depth using a Super Sharp blade. A corneal lamellar dissection was performed to create a semi-circle area. The cornea was flapped over but remained attached, and either a 3.0-mm or a 1.5-mm trephine opening was made centrally in the dissected cornea. The front plate was placed at 50% depth in the dissected corneal stroma with extension of the stem into the anterior chamber of the rabbit's eye. The corneal flap was pulled over the B-KPro front piece and sutured in place using six 10-0 nylon sutures. Immediately post-operatively and daily for two subsequent days, topical antibiotic polymyxin B/trimethoprim ophthalmic solution and a topical steroid, prednisolone acetate 1% ophthalmic suspension, were given. (B-KPro-FP-L, n = 1; B-KPro-FP-S, n = 2)

**2.11.4 B-KPro Type I with corneal autograft reactivity model in the rabbit—**The rabbit's cornea was cut with an 8.5 mm trephine blade and the corneal button was excised with corneal scissors. The autograft cornea was placed in a Teflon well, and a 3.0 mm trephine opening was made with an Acu-Punch centrally. The keratoprosthesis front part was placed upside-down, the corneal graft was slid over the stem, and the backplate was positioned over the stem and lightly screwed on until resistance was met. Viscoelastics and the titanium C-locking ring were not used as in routine B-KPro surgeries to avoid confounding material variables. Finally, the graft with its prosthesis was placed in the trephine opening. The surgical wound was closed with 12 interrupted 10-0 black monofilament nylon sutures equally spaced, and the knots were buried. PolymyxinB/trimethoprim drops but no steroids were given during the procedure, and no contact lens was placed. A lateral partial tarsorrhaphy using three interrupted 6-0 coated Vicryl sutures were placed and removed within three days. Immediately post-operatively and daily until one week prior to the end of the experiment, topical antibiotic polymyxinB/trimethoprim ophthalmic solution was given. A topical steroid, prednisolone acetate 1% ophthalmic suspension, was given immediately post-operatively and daily for one month in the pilot PMMA B-KPro only experiment and daily for 7 post-operative days in the HMPEI-PMMA compared to PMMA experiment. (PMMA B-KPRo, n = 2; HMPEI-PMMA B-KPro, n = 1)

**2.11.5 Contact lens corneal epithelium reactivity model in the rabbit—**Due to the epithelial overgrowth seen in the B-KPro model above and to assess the isolated epithelium's tissue response to HMPEI-coated materials, two different contact lenses were evaluated. The Kontur Precision Sphere (45% methafilcon, 55% water) is an extended wear soft clear bandage contact lens used for B-KPro [32]. The base diameter was 16 mm with an 8.6 - 9.8 mm base curve. In addition, a daily wear single use contact lens (Focus Dailies) composed of nelfilcon A (13.8 mm, 8.6 mm base curve) was used. (methafilcon contact lens, n = 3 sets; nelfilcon A contact lens, n = 3 sets)

Contact lenses were sterilized with ethylene oxide in a dry state and rehydrated with BSS solution for 15-30 min prior to placement. The rabbit's eye was sterilized with 5% povidone-iodine for 5 min and rinsed with sterile BSS solution to remove residual povidone-iodine. The contact lens or contact lens fragments were placed on to the corneal surface. A ¾ partial tarsorrhaphy with four 6-0 Vicryl sutures were used to prevent loss of the contact lenses from the rabbit's cornea surface. In a pilot study, the eye was examined at 2, 7, 14, and 22 days with re-suturing of the partial tarsorrhaphy. In subsequent experiments, the cornea surface was only examined at 22 days to minimize movement of the contact lenses. Any corneal defects were further examined with fluorescein (Flour1-StripA′1″, Wyeth-Ayerst Laboratories, Philadelphia, PA).

## 3. Results

### 3.1 *In vitro* Studies

Since there is suggestive evidence that ocular infection may be caused by a subset of organisms that possess virulence traits [20-22] and because media composition affects *in vitro* biofilm production [33], we evaluated *S. aureus* laboratory strains and clinical isolates for biofilm production under various media and growth conditions (Table 1). As others [34], we found that *S. aureus* ocular isolates formed biofilms variably under different conditions. We selected those ocular-associated strains that formed robust biofilms under diverse *in vitro* media and growth conditions (Table 1) for further studies. Our hyperbiofilm laboratory mutant, MN8m, avidly self-adhered but its adherence to polystyrene was variable depending on growth conditions. Since our ocular and mucosal surface isolates formed biofilms most robustly in BHI-2% sucrose, this medium was used for subsequent studies.

We examined both branched and linear DMPEIs. Unfortunately, both branched and linear DMPEIs painted on the surface of PMMA chipped under our biofilm growth conditions. Based on this finding and results of previous studies [19], in all subsequent experiments HMPEI ($C_6$) covalently attached to PMMA and titanium was employed.

Three different ocular-associated *S. aureus* isolates, a hyperbiofilm strain (MN8m), and a biofilm-defective strain (MN8mΔ*ica*(*x02237*)*tet)* were grown on both HMPEI-coated and parent materials (1-cm PMMA and Ti discs) for 24 h and 6 days. As seen in Figs. 2A and 2B for HMPEI-PMMA and PMMA (similar data for titanium not shown), marked inhibition of bacterial biofilms in all clinical isolates was observed by confocal laser scanning microscopy. There was >99% inhibition of both the laboratory-derived MN8m [14,25] and the biofilm-defective MN8m(Δ) strains by the derivatized materials. Due to the autofluorescence of acridine orange stained HMPEI-coated materials, a third channel was added (633 nm, Cy6-blue) for qualitative assessment. An accurate measurement of biofilm thickness and height was limited by the focal length required to measure mature biofilms grown on 150-200 micron discs within a tissue culture dish and the autoflourescence of HMPEI itself. Nevertheless, there was at least a 4- to 8-fold inhibition in *S. aureus* biofilm thickness on HMPEI-PMMA (Fig. 2A) compared to that on parent PMMA (Fig. 2B). There was likewise a 2- to 4-fold less biofilm formation on HMPEI-Ti materials compared to that on parent Ti (note that our *S. aureus* strains preferentially grew biofilms on parent PMMA compared to parent Ti).

Biofilm formation and adherence by the three ocular *S. aureus* isolates, a hyperbiofilm strain (MN8m), and a MN8mΔ *ica*(*x02237*)*tet* defective biofilm grown on HMPEI-PMMA discs compared to those on unmodified PMMA discs were then examined by SEM. The inhibition of biofilm formation persisted in all isolates after 6 days of continuous static growth on HMPEI-PMMA (Fig. 2C), while the bacteria grown on parent PMMA continued to accumulate more mature biofilm structures (Fig. 2D). In addition, lysis of bacterial cell

walls resulting in sickled shaped cells was observed on HMPEI-PMMA discs (Fig. 2C). The hyperbiofilm forming strain (Fig. 2E) and the biofilm-defective strain showed >99% biofilm inhibition when grown on HMPEI-PMMA discs compared to unmodified PMMA discs. The only bacteria that remained intact appeared to be suspended in a bacterial-derived matrix and not in contact with the coated HMPEI-PMMA material below (Fig. 2E).

To screen for cytotoxicity *in vitro*, HMPEI-PMMA discs were compared to the uncoated PMMA counterparts by placing both on confluent immortalized human corneal limbal epithelial (HCLE) cells. HMPEI-PMMA exhibited no additional toxicity (Fig. 3A) in comparison to PMMA (Fig. 3B) for HCLE cells. Similar morphological disruption of the stratified HCLE cells after placement of unadhered discs was seen in both HMPEI-PMMA and parent PMMA discs after the first 48 h, and similar epithelial cell growth and recovery was seen on HMPEI-PMMA and PMMA discs comparable to the HCLE cell (no disc) control by 72 h (Figs. 3A, 3B, and 3C). Rose bengal staining demonstrated equal stratification of HCLE cells grown on HMPEI-PMMA and PMMA discs and comparable to HCLE cell (no disc) control (data not shown).

Quantitative assessment of lysed HCLE cells by a lactate dehydrogenase release cytotoxicity assay showed no additional cell cytotoxicity in the case of HMPEI-PMMA discs compared to PMMA controls at 24 h, and there was significantly less cytotoxicity seen on HMPEI-PMMA discs compared to the control PMMA discs by 48 and 72 h (Fig. 3D) ($p$ values < 0.0001 and <0.01, respectively). Less cell cytotoxicity was seen with the HCLE cell only (no disc) control compared to either HMPEI-PMMA or PMMA at 24 and 48 hours, but more cell cytotoxicity was measured at 72 hours due to cell crowding and nutritional limitations (data not shown).

Finally, it is noteworthy that the covalent attachment of HMPEI to B-KPro did not alter its optical clarity or refractive optical power.

### 3.2 *In vivo* Evaluation

Since the B-KPro is predominantly in contact with the corneal stroma, this model was designed to evaluate for any toxicity within the corneal stroma of the rabbit (Fig. 4A). There was less corneal inflammatory response with HMPEI-PMMA discs than with parent PMMA ones in both BALB/c mice (data not shown; N = 4 for 1-mm discs) and New Zealand white rabbits (Fig. 5; N = 4 for 3-mm PMMA discs; N = 3 for 1.5-mm PMMA discs). There was also less corneal edema, corneal haze, neovascularization, and conjunctival irritation and discharge seen with HMPEI-PMMA 3-mm discs (Fig. 5A) compared to the control ones (Fig. 5B) intrastromally (Table 2). Histopathology revealed that intrastromal HMPEI-PMMA discs showed no more inflammation than unmodified PMMA ones, whether they were surgically removed or spontaneously extruded.

HMPEI-Ti discs (Fig. 5C; N = 4) when compared to parent Ti controls (Fig. 5D; N = 4) exhibited no more reactivity by clinical assessment. The histopathologic examination of the titanium discs after 61 days showed an excellent host stromal tolerance both with HMPEI coating and without (Figs. 8A and 8B, respectively). There was no evidence of inflammation, vascularization, or active scar formation (Figs. 8A and 8B). Scanning electron microscopy of the HMPEI-Ti discs and parent Ti discs (Figs. 9A and 9B, respectively, 25X, inset 500X) extracted from the corneal stroma at 61 days revealed no inflammatory response to either. In addition, denser, more compact, and confluent cells were seen on HMPEI-Ti discs (Fig. 9A) than on parent Ti discs (Fig. 9B).

Note that HMPEI-PMMA discs were no more reactive than the parent PMMA ones when placed in the anterior chamber of the eye. Although the reactivity was greater in the anterior

chamber model than in the intrastromal one (data not shown), the unpredictable free-floating movement of the discs within the anterior chamber limited this model's usefulness.

Using a Keratoprosthesis front piece (KPro-FP) placed into the corneal stroma and the stem extending into the anterior chamber (Fig. 4B), the reactivity in the rabbit was assessed over time. On post-operative day 2, HMPEI-PMMA KPro-FP (Fig. 6A) appeared similar to control PMMA KPro-FP (Fig. 6B), with the exception of the onset of iritis in PMMA KPro-FP. There was less corneal edema, haze, neovascularization, conical ectasia, and conjunctival discharge in HMPEI-PMMA KPro-FP (Fig. 6C) compared to parent PMMA KPro-FP (Fig. 6D) by post-operative day 30. By three months, these changes progressed further in the PMMA KPro-FP (Fig. 6F, Table 2), while the HMPEI-PMMA KPro-FP remained relatively unchanged (Fig. 6E, Table 2). Small retroprosthetic membranes formed on both PMMA and HMPEI-PMMA stems. Front pieces were surgically extracted on post-operative day 105. The histopathologic examination of PMMA front pieces with and without HMPEI coating revealed different host stromal responses. The HMPEI-coated specimen showed a fibroblast reparation response surrounding the posterior aspect of the implant front piece without inflammation or vascularization (Fig. 8C). The non-coated front piece displayed moderate acute inflammation with minimal microvascularization (Fig. 8D). SEM showed denser, more compact and confluent cells attached to HMPEI KPro-FP (Fig. 9C), as compared to looser, disorganized cells attached to the control PMMA KPro-FP (Fig. 9D).

To assess what effect the HMPEI coating may have on the epithelial layer, stroma, endothelium, anterior chamber, and the corneal graft healing, a human-sized B-KPro Type I with a corneal autograft was placed in a rabbit eye with less topical steroid usage. When HMPEI-PMMA B-KPro (Figs. 7A and 7C) is compared to the uncoated PMMA B-KPro at postoperative day 69 (Figs. 7B and 7D) in the rabbit, less corneal edema, haze, and conjunctival discharge is observed (Table 2). As seen with the KPro-FP model on the side view, the control PMMA B-KPro underwent conical ectasia of the cornea (Fig. 9D) that was not observed in the HMPEI B-KPro in the rabbit. This conical reshaping of the cornea is unique to the rabbit and not seen in humans with a B-KPro. In addition, epithelial growth on the front piece was seen with HMPEI-PMMA B-KPro (Figs. 7A and 7C), while it did not occur on control PMMA B-KPro surfaces (Figs. 7B and 7D) in the rabbit (nor does it occur normally on PMMA front piece surfaces in humans [35]). Even with mechanical removal of the epithelial growth, the epithelium re-grew within one month.

To evaluate the epithelial overgrowth seen on HMPEI-PMMA B-KPro, we determined whether this was a HMPEI-specific response by covalently attaching HMPEI to two different contact lenses (methafilcon and netilicon) and comparing the results to those seen with the parent materials. We did observe epithelial overgrowth and possibly enhanced adherence with associated epithelial defects with both HMPEI-netilicon and HMPEI-methafilcon contact lenses by day 22 in the rabbit. This phenomenon was not seen in the control contact lenses in the rabbit. On histopathological examination, there was epithelial overgrowth occurring where the contact lens space was (not shown). SEM demonstrated the normal mosaic of light, medium, and dark epithelial cell organization (Fig. 9E) and the presence of microplicae (Fig. 9F).

The drying effects associated with our covalent modification may have adversely affected the high water content and/or decreased $O_2$ permeability of the soft contact lenses. Note, however, that the purpose of this additional evaluation was to assess HMPEI-associated epithelial overgrowth on material(s) known to reside on the epithelial surface that are normally resistant to epithelial overgrowth, and not to determine HMPEI's feasibility for contact lens use.

## 4. Discussion

Immobilized HMPEI exerts its antimicrobial effects by long hydrophobic polycationic chains that are able to penetrate and lyse the cell membranes/walls of microorganisms [14, 15]. This contact-dependent killing has been demonstrated for planktonic bacteria, as well as viruses and fungi [17-19], but heretofore not for bacterial biofilms that are the major cause of device-associated infections [3] and naturally resistant to antimicrobial agents [5]. Using large inocula ($>10^7$) of *S. aureus* biofilm-forming clinical isolates, we determined herein that the surface derivatization with the hydrophobic polycation brought about a drastic reduction of biofilm formation and a sustained bacterial killing over at least one week in continuous growing cultures *in vitro*.

The function of B-KPro, an artificial cornea, depends on its optical clarity and refraction. By optical bench testing, we determined that covalent modification with HMPEI did not alter B-KPro's shape, clarity, refractive index, or image-forming quality. We also determined that HMPEI covalently attached to PMMA conferred no additional cell cytotoxicity or abnormal morphological changes on immortalized human corneal epithelial cells (HCLE), compared to those observed with control PMMA. There were no observable untoward effects on epithelial cell attachment, stratification, differentiation, or proliferation, as compared to PMMA itself. Despite the inherent limitations of 2-D tissue culture models in the study of 3-D materials, we believe that it served as a useful screen for cytotoxic effects of comparative materials with similar physical properties [36]. The results obtained herein support previously reported lack of toxicity with monkey kidney cells [16].

In multiple eye compartments in the rabbit *in vivo*, there was no more host tissue reactivity or inflammation observed with HMPEI-derivatized materials, as compared to the controls, observed by clinical assessment, histopathologic examination, and SEM. In fact, in both the intrastromal-anterior chamber model and the B-KPro model, the clinical tissue reactivity (corneal swelling and neovascularization) appeared less by the first week post-operatively with HMPEI-PMMA materials than with the uncoated controls. Also, by histopathologic examination and SEM, HMPEI-coated materials showed no more inflammation and more continuous cellular coatings without conspicuous debris than the parent materials.

The B-KPro front plate is composed of PMMA that normally inhibits epithelial overgrowth over the polished optical center in both humans and rabbits. Interestingly, we observed epithelial overgrowth on HMPEI-coated PMMA B-KPro not seen on the uncoated one. Although this overgrowth may obscure vision and is generally undesirable [35], organized corneal epithelial growth and differentiation might form a smooth refractive surface and a protective tight junctional barrier that prevents decreases in net fluid transport out from the stroma and corneal penetration by pathogens [37]. Thus epithelial overgrowth on the B-KPro front plate may be of value in prevention of inflammation and infection, particularly in resource-poor areas of the world, and warrants further investigation.

The results of the *in vivo* biocompatibility evaluations conducted in this work are further strengthened by the fact that the rabbit eye is generally more sensitive than the human eye [39]. The rabbit cornea is thinner with a steeper curvature and is more susceptible to evaporative damage because of a slower blink frequency than a human eye [38]. It also has a heightened tissue response to minor surgical procedures, foreign materials, drugs, or chemicals [38]. Another factor strengthening our findings is that topical corticosteroids were given only for a few days postoperatively; standard clinical postoperative regimens might have masked inflammation in our rabbit experiments. In addition, the rabbit eye readily extrudes foreign material, limiting long-term studies beyond a few months [39]. Thus we

believe that the present work is an important step toward testing these HMPEI-coated materials in humans.

## 5. Conclusions

HMPEI covalently attached to B-KPro materials inhibits biofilm formation by *S. aureus*. The immobilized hydrophobic polycation confers no additional toxicity or reactivity compared to the control *in vitro* or *in vivo* in enucleated eyeballs in the adjacent corneal stroma, anterior chamber, or iris. Because it is easily observable and the prosthetic material can be easily removed or exchanged, the B-KPro may represent an ideal format for testing these antimicrobial coatings in humans.

## Acknowledgments

We thank Therese F. Labrecque, M. Susan Parker, Rick P. Boody, David W. Sheridan, and Nancy Sutcliffe (MEEI Henry Whittier Porter Bacteriology Laboratory); Donald Pottle (SERI Confocal Microscopy facility); Sandra J. Spurr-Michaud (SERI - tissue culture); Norman A. Michaud and Valdemar Araujo (MEEI Core Morphology); John M. Graney (JG Machine, Woburn, MA); Kathryn V. Martin (MEEI animal research assistance); Marcus Rauch, Susan R. Heimer, James Chodosh, Roberto Pineda II, and the MEEI B-KPro Research Group; as well as Larisa Gelfand and Rhonda Walcott-Harris (MEEI) for administrative assistance; Andrew Wright (Molecular Biology and Microbiology, Tufts School of Medicine, Boston, MA) for critical review of the manuscript; and Harris K. Liu and Roger Nassar (MIT) for help with the manuscript.

This work was made possible by the generous support of Fight for Sight Grant-In-Aid (I.B.), MEEI B-KPro Fund, Institute for Soldier Nanotechnologies at MIT under contract through the U.S. Army Research Office DAAD-19-D-0002 (A.M.K.), and NIH grant EY017381 (M.S.G.).

## References

1. Butany J, Collins MJ. Analysis of prosthetic cardiac devices: a guide for the practicing pathologist. J Clin Pathol. 2005; 58:113–124. [PubMed: 15677529]
2. Baker, AS.; Schein, OD. Ocular infections. In: Bisno, AL.; Waldvogel, FA., editors. Infections associated with indwelling medical devices. ASM Press; Washington, D.C.: 1989. p. 75-92.
3. Darouiche RO. Treatment of infections associated with surgical implants. N Engl J Med. 2004; 350:1422–1429. [PubMed: 15070792]
4. Scott, RD, II. The direct medical costs of healthcare-associated infections in U.S. hospitals and the benefits of prevention. CDC 2009. [cited 20April2011]; [16 screens]. Available from URL: www.cdc.gov/ncidod/dhqp/pdf/Scott_CostPaper.pdf
5. Costerton JW, Stewart PS, Greenberg EP. Bacterial biofilms: a common cause of persistent infections. Science. 1999; 284:1318–1322. [PubMed: 10334980]
6. Fux CA, Costerton JW, Stewart PS, Stoodley P. Survival strategies of infectious biofilms. Trends in Microbiology. 2005; 13:34–39. [PubMed: 15639630]
7. Behlau I, Gilmore MS. Microbial biofilms in ophthalmology and infectious diseases. Arch Ophthalmol. 2008; 126:1572–1581. [PubMed: 19001227]
8. Dohlman CH, Harissi-Dagher M, Khan BF, Sippel K, Aquavella JV, Graney JM. Introduction to the use of the Boston keratoprosthesis. Expert Rev Ophthalmol. 2006; 1:41–48.
9. Harissi-Dagher M, Khan BF, Schaumberg DA, Dohlman CH. Importance of nutrition to corneal grafts when used as a carrier of the Boston Keratoprosthesis. Cornea. 2007; 26:564–568. [PubMed: 17525653]
10. Dohlman CH, Dudenhofer EJ, Khan BF, Morneault S. Protection of the ocular surface after keratoprosthesis surgery: the role of soft contact lenses. CLAO J. 2002; 28:72–74. [PubMed: 12054373]
11. Durand ML, Dohlman CH. Successful prevention of bacterial endophthalmitis in eyes with the Boston keratoprosthesis. Cornea. 2009; 28:896–901. [PubMed: 19654525]

12. Pineda R II, Ament JD, Tilahun Y, Behlau I, Dohlman CH. Prospective evaluation of sustaining the Boston Keratoprosthesis in the developing world: a pilot study. Invest Ophthalmol Vis Sci. 2009; 50 ARVO E-Abstract 1497. Available at URL: www.iovs.org.
13. Bennett-Guerrero E, Pappas TN, Koltun WA, Fleshman JW, Lin M, Garg J, et al. for the SWIPE 2 Trial Group. Gentamicin-collagen sponge for infection prophylaxis in colorectal surgery. N Engl J Med. 2010; 363:1038–1049. [PubMed: 20825316]
14. Lewis K, Klibanov AM. Surpassing nature: rational design of sterile-surface materials. Trends Biotechnol. 2005; 23:343–348. [PubMed: 15922467]
15. Klibanov AM. Permanently microbicidal materials coatings. J Mater Chem. 2007; 17:2479–2482.
16. Milovic NM, Wang J, Lewis K, Klibanov AM. Immobilized *N*-alkylated polyethylenimine avidly kills bacteria by rupturing cell membranes with no resistance developed. Biotechnol Bioeng. 2005; 90:715–722. [PubMed: 15803464]
17. Lin J, Tiller JC, Lee SB, Lewis K, Klibanov AM. Insights into bactericidal action of surface-attached poly (vinyl-*N*-hexylpyridium) chains. Biotechnol Lett. 2002; 24:801–805.
18. Lin J, Qui S, Lewis K, Klibanov AM. Mechanism of bactericidal and fungicidal activities of textiles covalently modified with alkylated polyethylenimine. Biotechnol Bioeng. 2003; 83:168–172. [PubMed: 12768622]
19. Haldar J, An D, Alvarez de Cienfuegos L, Chen J, Klibanov AM. Polymeric coatings that inactivate both influenza virus and pathogenic bacteria. Proc Natl Acad Sci USA. 2006; 103:17667–17671. [PubMed: 17101983]
20. Booth MC, Hatter KL, Miller D, Davis J, Kowalski R, Parks DW, et al. Molecular epidemiology of *Staphylococcus aureus* and *Enterococcus faecalis* in endophthalmitis. Infect Immun. 1998; 66:356–360. [PubMed: 9423880]
21. Behlau, I.; Leonard, EM.; Heimer, SR.; Martin, JN.; Dohlman, CH.; Gilmore, MS. Characterization of keratitis-associated *Staphylococcus aureus* infections from the Boston area. Ocular Microbiol Immunol Group. 2008. E-Abstract 14. Available at URL: http://eyemicrobiology.upmc.com/2008.Abstracts/2008OMIGAbstract14.html
22. Behlau I, Heimer SR, Leonard EM, Martin JN, Dohlman CH, Gilmore MS. *Staphylococcus aureus*-associated keratitis: phenotypic and genotypic characterization. Invest Ophthalmol Vis Sci. 2009; 50 ARVO E-Abstract 5113. Available at URL: www.iovs.org.
23. Lowy FD. *Staphylococcus aureus* infections. N Engl J Med. 1998; 339:520–532. [PubMed: 9709046]
24. Ciolino JB, Hoare TR, Iwata NG, Behlau I, Dohlman CH, Langer R, et al. Drug-eluting contact lens. Invest Ophthalmol Vis Sci. 2009; 50:3346–3352. [PubMed: 19136709]
25. Jefferson KK, Cramton SE, Götz F, Pier GB. Identification of a 5-nucleotide sequence that controls expression of the *ica* locus in *Staphylococcus aureus* and characterization of the DNA-binding properties of IcaR. Molec Microbiol. 2003; 48:889–899. [PubMed: 12753184]
26. Schlievert PM, Blomster DA. Production of staphylococcal pyrogenic exotoxin type C: influence of physical and chemical factors. J Infect Dis. 1983; 147:236–242. [PubMed: 6827140]
27. Clinical and Laboratory Standards Institute. M7–A7, Methods for dilution antimicrobial susceptibility tests for bacteria that grow aerobically – approved standard-seventh edition. CSLI; Wayne, PA: 2006.
28. Ito Y, Imanishi Y, Yonezawa K, Kasuga M. Protein-free cell culture on an artificial substrate with covalently immobilized insulin. Proc Natl Acad Sci USA. 1996; 93:3598–3601. [PubMed: 8622981]
29. Nanci A, Wuest JD, Péru L, Brunet P, Sharma V, Zalzal S, McKee MD. Chemical modification of titanium surfaces for covalent attachment of biological molecules. J Biomed Mater Res. 1998; 40:324–335. [PubMed: 9549628]
30. Christensen GD, Simpson WA, Younger JJ, Baddour LM, Barrett FF, Melton DM, Beachey EH. Adherence of coagulase-negative staphylococci to plastic tissue culture plates: a quantitative model for the adherence of staphylococci to medical devices. J Clin Microbiol. 1985; 22:996–1006. [PubMed: 3905855]

31. Argueso P, Tisdale A, Spurr-Michaud S, Sumiyoshi M, Gipson IK. Mucin characteristics of human corneal-limbal epithelial cells that exclude the rose bengal anionic dye. Invest Ophthalmol Vis Sci. 2006; 47:113–119. [PubMed: 16384952]
32. Harissi-Dagher M, Beyer J, Dohlman CH. The role of soft contact lenses as an adjunct to the Boston keratoprosthesis. Int Ophthalmol Clin. 2008; 48:43–51. [PubMed: 18427260]
33. Rice SA, Koh KS, Queck SY, Labbate M, Lam KW, Kjelleberg S. Biofilm formation and sloughing in *Serratia marcescens* are controlled by quorum sensing and nutrient cues. J Bacteriol. 2005; 187:3477–3485. [PubMed: 15866935]
34. Seidl K, Goerke C, Wolz C, Mack D, Berger-Bächi B, Bischoff M. *Staphylococcus aureus* CcpA affects biofilm formation. Infect Immunity. 2008; 76:2044–2050. [PubMed: 18347047]
35. Khalifa YM, Davis D, Mamalis N, Moshirfar M. Epithelial growth over the optic surface of the type 1 Boston Keratoprosthesis: histopathology and implications for biointegration. Clin Opthalmol. 2010; 4:1069–1071.
36. Shimizu K, Kobayakawa S, Tsuji A, Tochikubo T. Biofilm formation on hydrophilic intraocular lens material. Curr Eye Res. 2006; 31:989–997. [PubMed: 17169836]
37. Lu L, Renach PS, Kao WWY. Corneal epithelial wound healing. Exp Biol Med. 2001; 226:653–664.
38. Wilhelmus KR. The Draize eye test. Surv Ophthalmol. 2001; 45:493–515. [PubMed: 11425356]
39. Espana EM, Acosta AC, Stoiber J, Fernandez V, Lamar PD, Villain FL, et al. Long-term follow-up of a supradescemetic keratoprosthesis in rabbits: an immunofluorescence study. Graefes Arch Clin Exp Ophthalmol. 2011; 249:253–260. [PubMed: 20814695]

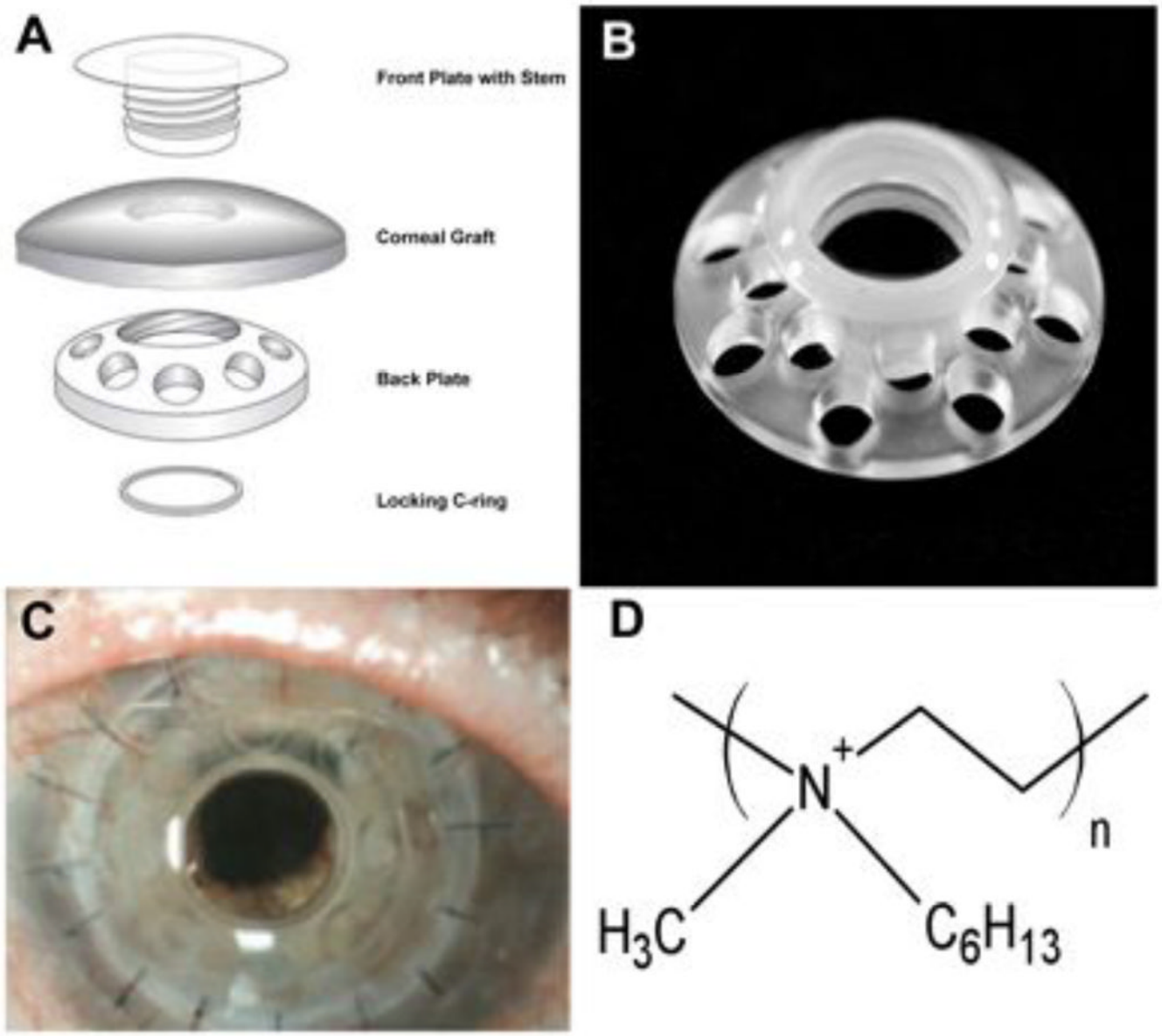


**Figure 1.**

(**A**) Schematic diagram of the B-KPro composed of optical quality PMMA shaped like a collar-button and implanted into a corneal graft secured with a titanium locking ring. (**B**) Photograph of the B-KPro composed of PMMA. (**C**) Photograph of the B-KPro in a corneal allograft implanted in a patient and secured by 16 sutures. This patient had three previous standard corneal graft failures; visual acuity is now 20/25. (**D**) Chemical structure of long-chained, linear *N,N*-hexyl,methyl-polyethylenimine (HMPEI).

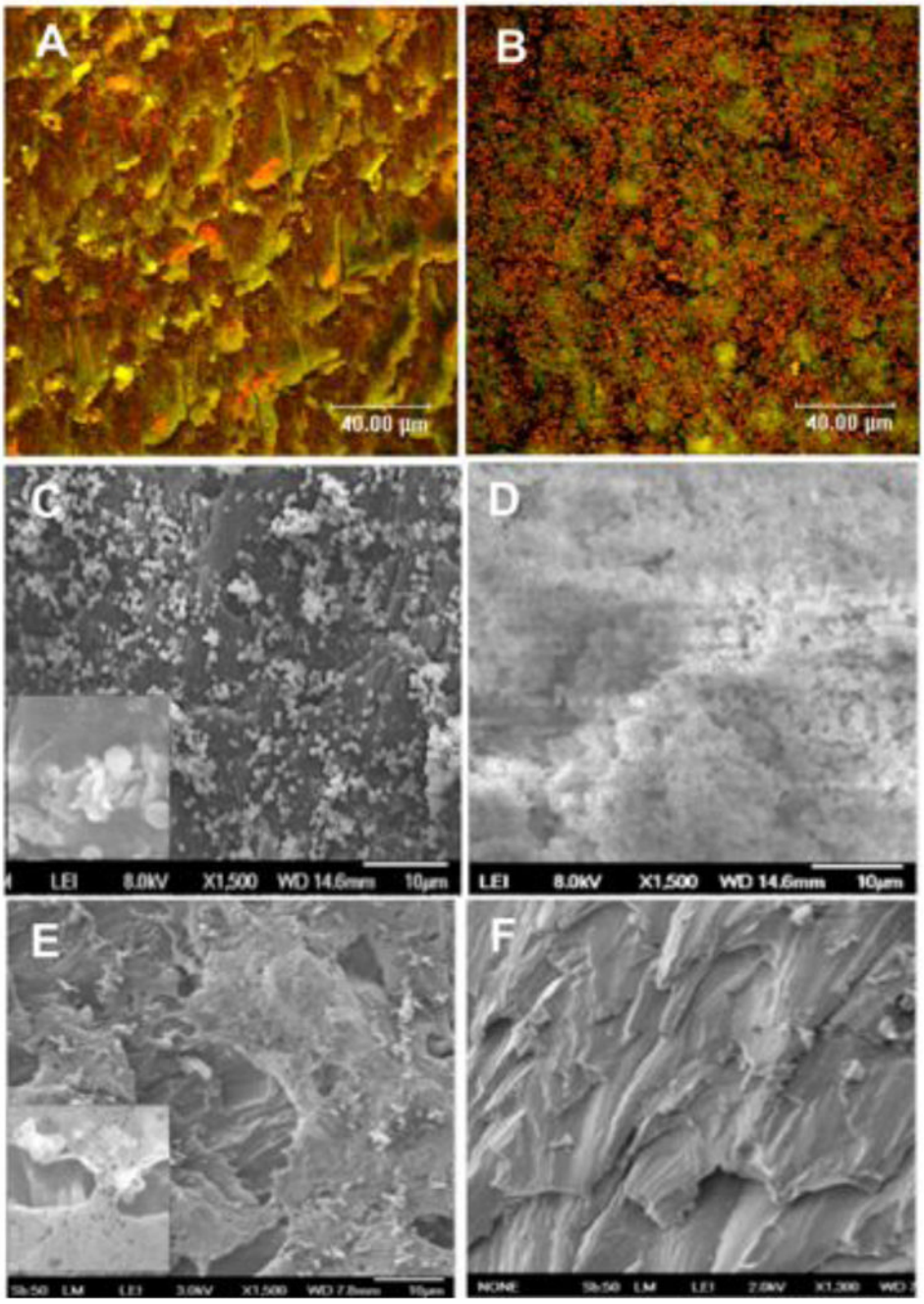


**Figure 2.**

(**A** and **B**) Confocal laser scanning micrographs of *S. aureus* derived from an eye canniculus infection (MEEI-IB013) after 20 h of static culture on a disc *in vitro*. *S. aureus* grown on HMPEI-PMMA discs shows few colonies or small microcolonies (**A**), while the bacteria grown on control PMMA discs forms thick, confluent biofilm structures (**B**). Bacteria appear orange (1 micron in size) (acridine orange stain; three-channel combination of 488, 568, and 633 nm) (63X). (**C, D**) Scanning electron micrographs of *S. aureus* derived from a keratitis infection (MEEI-IB001) after 6 days of continuous static growth *in vitro*. *S. aureus* grown on HMPEI-PMMA discs shows single or small microcolonies with lysis of bacterial

walls (1500X); inset shows higher magnification (5000X) of bacterial cell lysis (**C**). Confluent, mature bacterial biofilms are seen on control PMMA discs (1500X) (**D**). (**E**) SEM of laboratory-derived hyperbiofilm forming *S. aureus* strain (MN8m) after 6 days of continuous static growth on HMPEI-PMMA discs *in vitro*. *S. aureus* bacterial colonies are seen suspended on bacterial-derived extrapolysaccharide matrix, while no bacteria are seen on the HMPEI-PMMA disc below (1500X). Inset shows a higher magnification (4000X) of bacterial colonies suspended over HMPEI-PMMA material with lysis of bacterial walls on contact with it. (**F**) SEM of a no-bacteria control of HMPEI-PMMA discs. The rough cutting of PMMA disc is unaltered by covalent attachment of HMPEI to it (1300X).

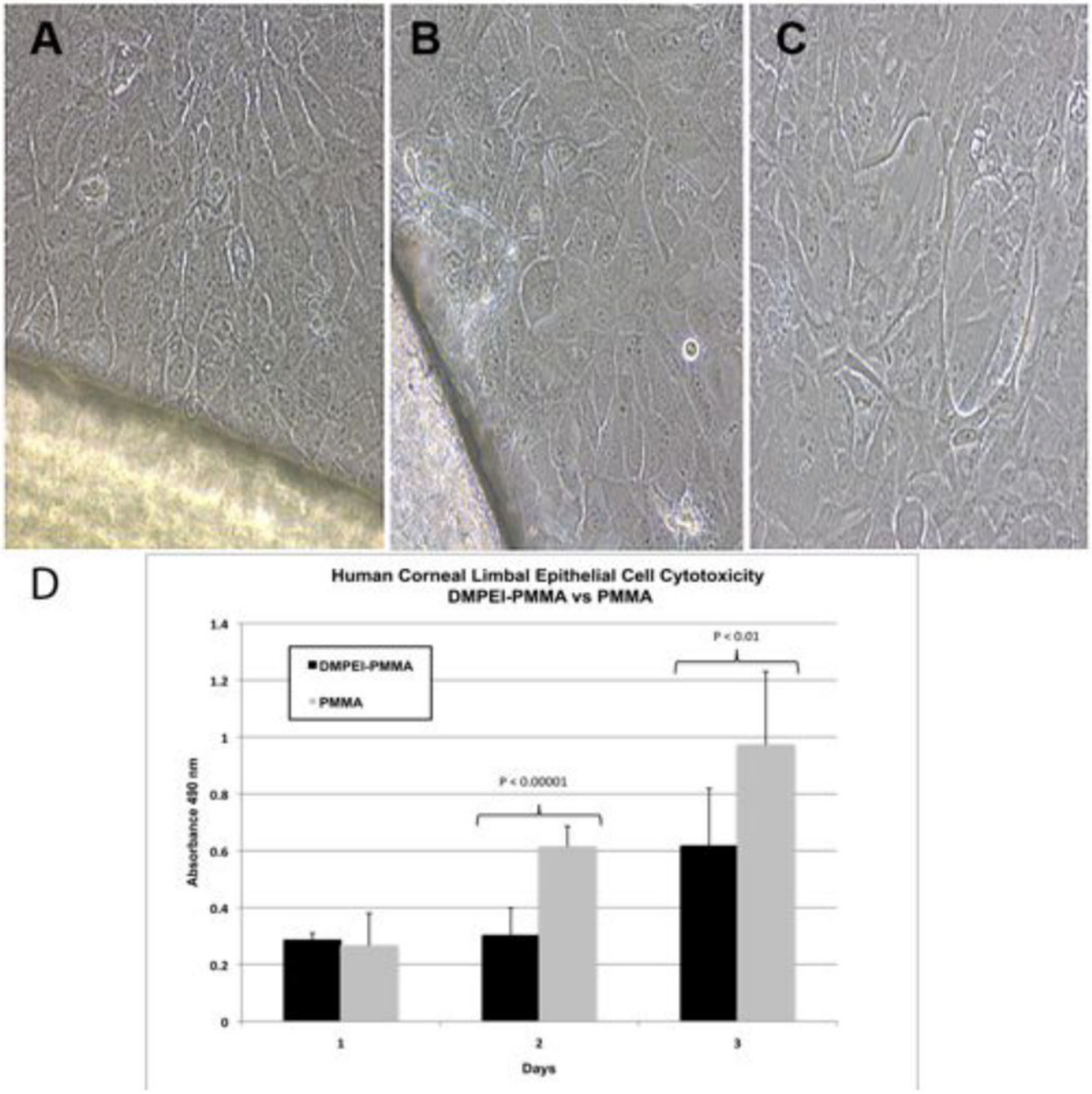


**Figure 3.**

Phase-contrast images of unstained immortalized human corneal epithelial (HCLE) cells grown on tissue culture dishes *in vitro* at 72 h after the addition of (**A**) HMPEI-PMMA disc, (**B**) control PMMA disc, and (**C**) no-disc control. There is no evidence of devitalization of the epithelial cells resulting from the HMPEI coating. (**D**) Graph shows HCLE cell cytotoxicity as measured by released lactate dehydrogenase associated with cell lysis. There is no more HCLE cell cytotoxicity measured with HMPEI-coated PMMA discs than with control PMMA ones at 24 h. There is statistically significantly less toxicity at 48 h and 72 h

with HMPEI-PMMA discs than with control PMMA discs ($p$ values <0.00001 and <0.01, respectively).

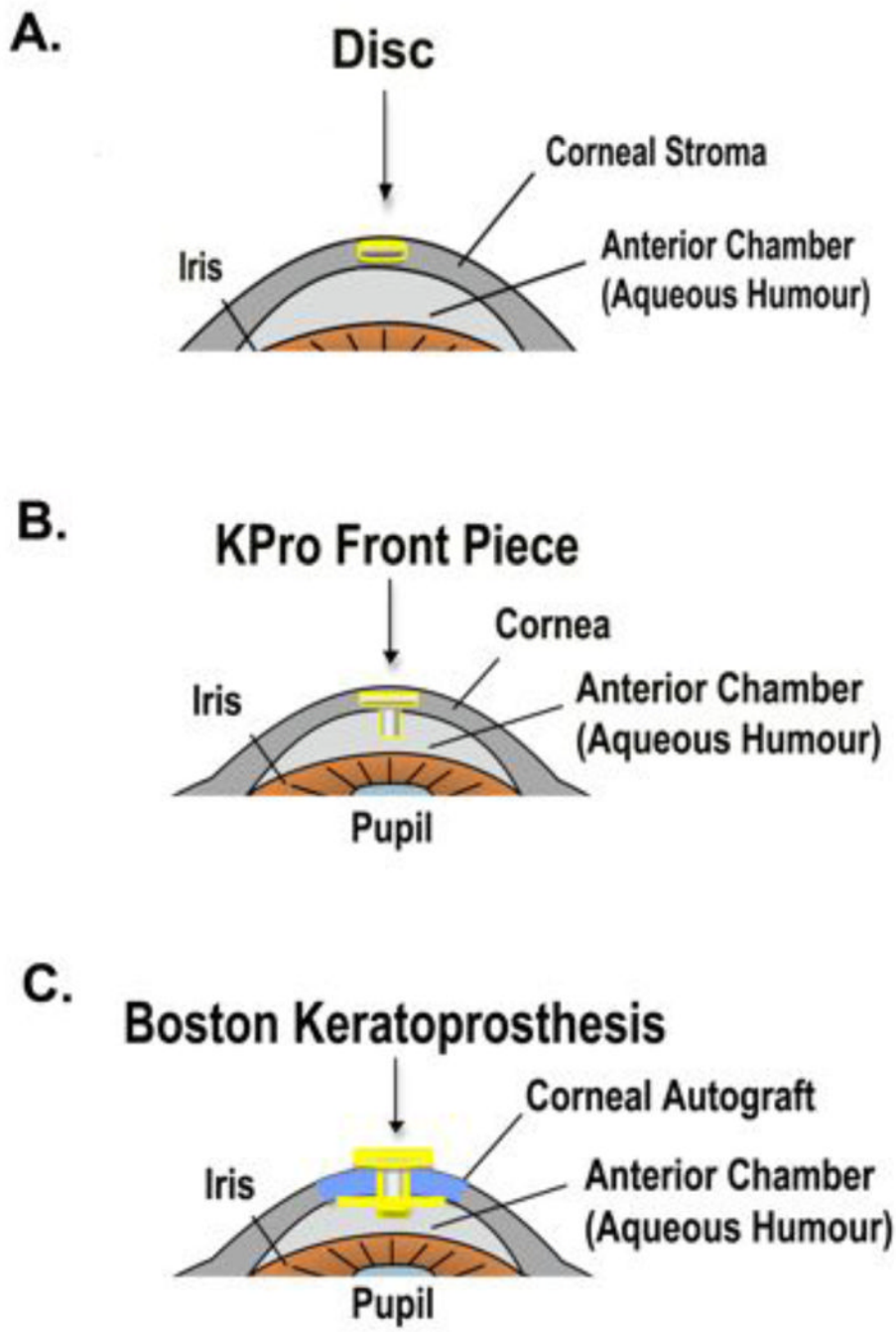


**Figure 4.**

Schematic diagrams of the various material models in the anterior eye of the rabbit. (**A**) The disc model shows the disc residing intrastromally in the cornea. (**B**) The KPro Front Piece (KPro-FP) model shows the front piece in the corneal stroma with its stem protruding into the anterior chamber. (**C**) The B-KPro model shows the PMMA front plate resting on the corneal epithelium with the PMMA stem extending through a corneal autograft, through a backplate, into the anterior chamber, and secured by a locking C-ring.

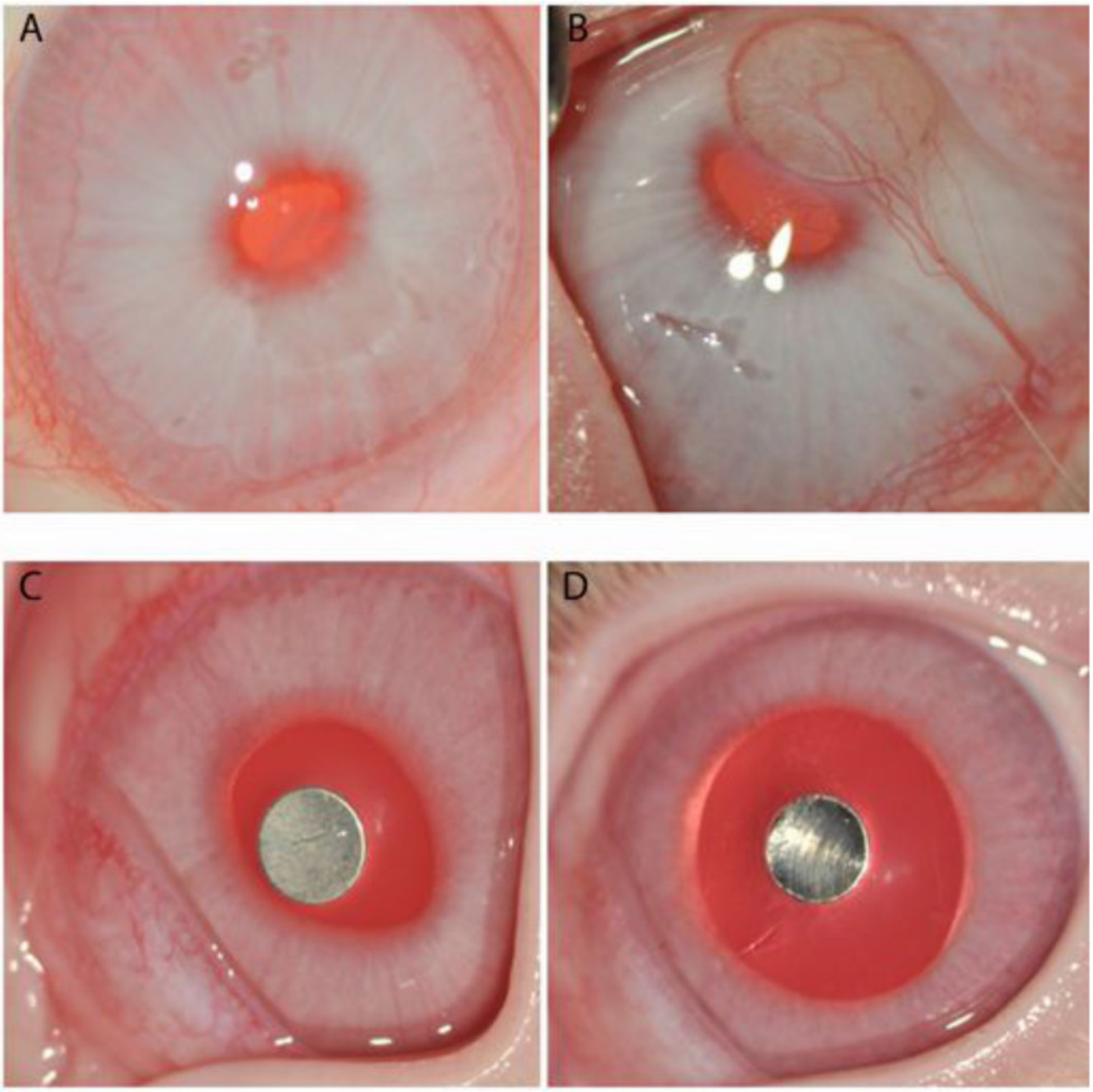


**Figure 5.**

Representative clinical photographs of 3-mm discs placed intrastromally within the cornea of the New Zealand white rabbit. (**A**) HMPEI-coated PMMA disc is compared to (**B**) control PMMA disc at 38 days postoperatively. (**A**) There is only a faint outer disc haze seen with the HMPEI-PMMA disc. (**B**) A white corneal nontransparent haze with corneal neovascularization is seen over the control PMMA disc. There is less corneal tissue reactivity with HMPEI-coated PMMA discs compared to control PMMA discs. Representative clinical photographs of (**C**) HMPEI- coated titanium disc placed

intrastromally compared to (**D**) control Ti counterpart at 61 days postoperatively shows minimal tissue reactivity and similar clinical features in both groups.

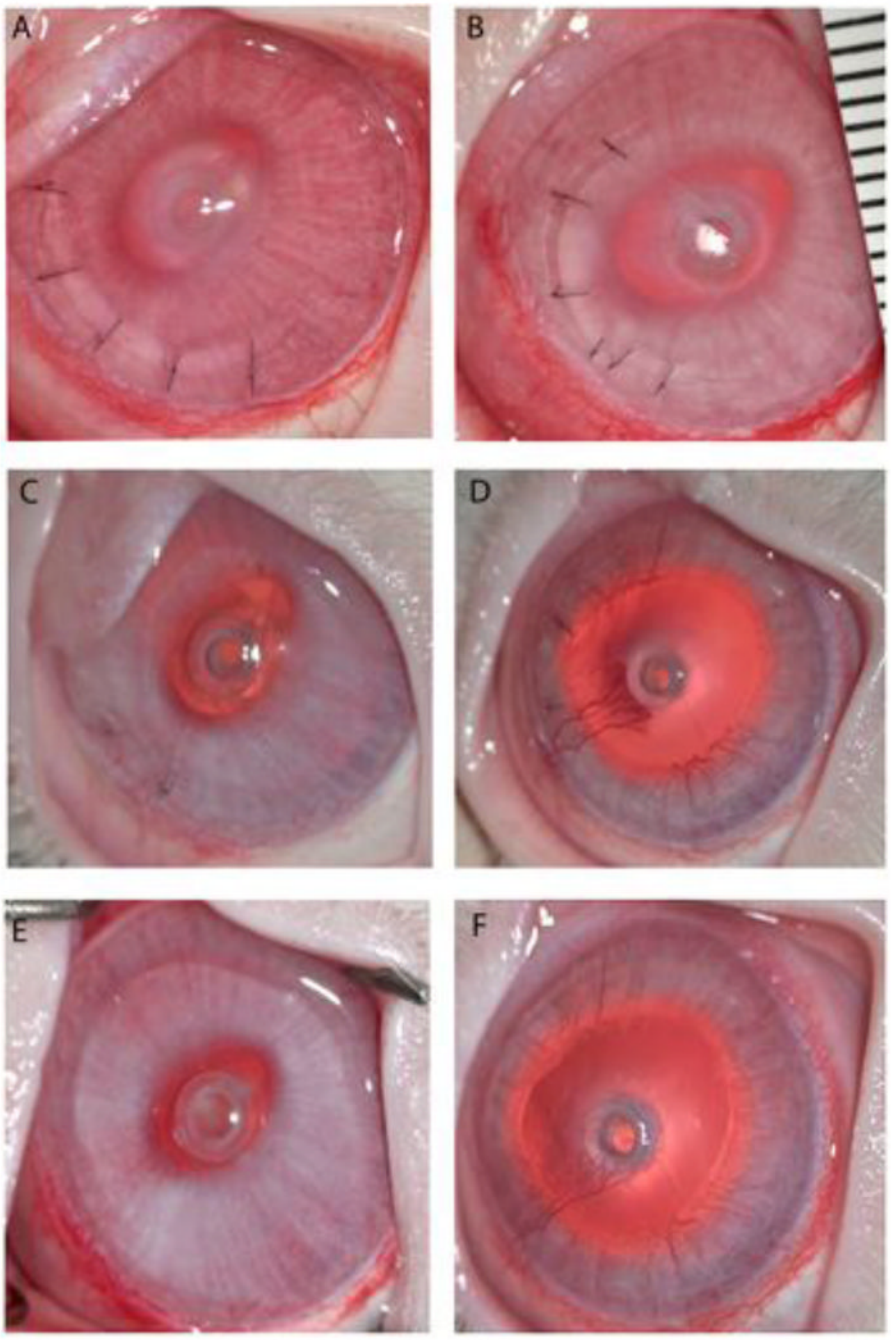


**Figure 6.**

Clinical photographs of comparative KPro-FP placed intrastromally with the extension into the anterior chamber of the eye of a New Zealand white rabbit shown at three representative time points. (**A, B**) At post-operative day 2, HMPEI-PMMA KPro-FP (**A**) rabbit eye shows a lamellar flap with 6 sutures and mild post-operative corneal swelling similar to control PMMA KPro-FP (**B**) showing the same clinical features. (**C, D**) At one month post-operatively, HMPEI-PMMA KPro-FP (**C**) shows minimal corneal swelling, only a mild neovascularization at the surgical wound site, and no corneal ectasia, while PMMA KPro-FP (**D**) shows moderate corneal edema, corneal neovascularization has advanced to the front

plate, and there is mild corneal ectasia. (**E, F**) By three months post-operatively, HMPEI-PMMA KPro-FP (**E**) remains quiescent with minimal corneal reactivity, neovascularization, and conical ectasia compared to the uncoated control PMMA KPro-FP (**F**) that shows moderate corneal swelling, extension of the corneal neovascularization over the front piece, and progressive conical ectasia.

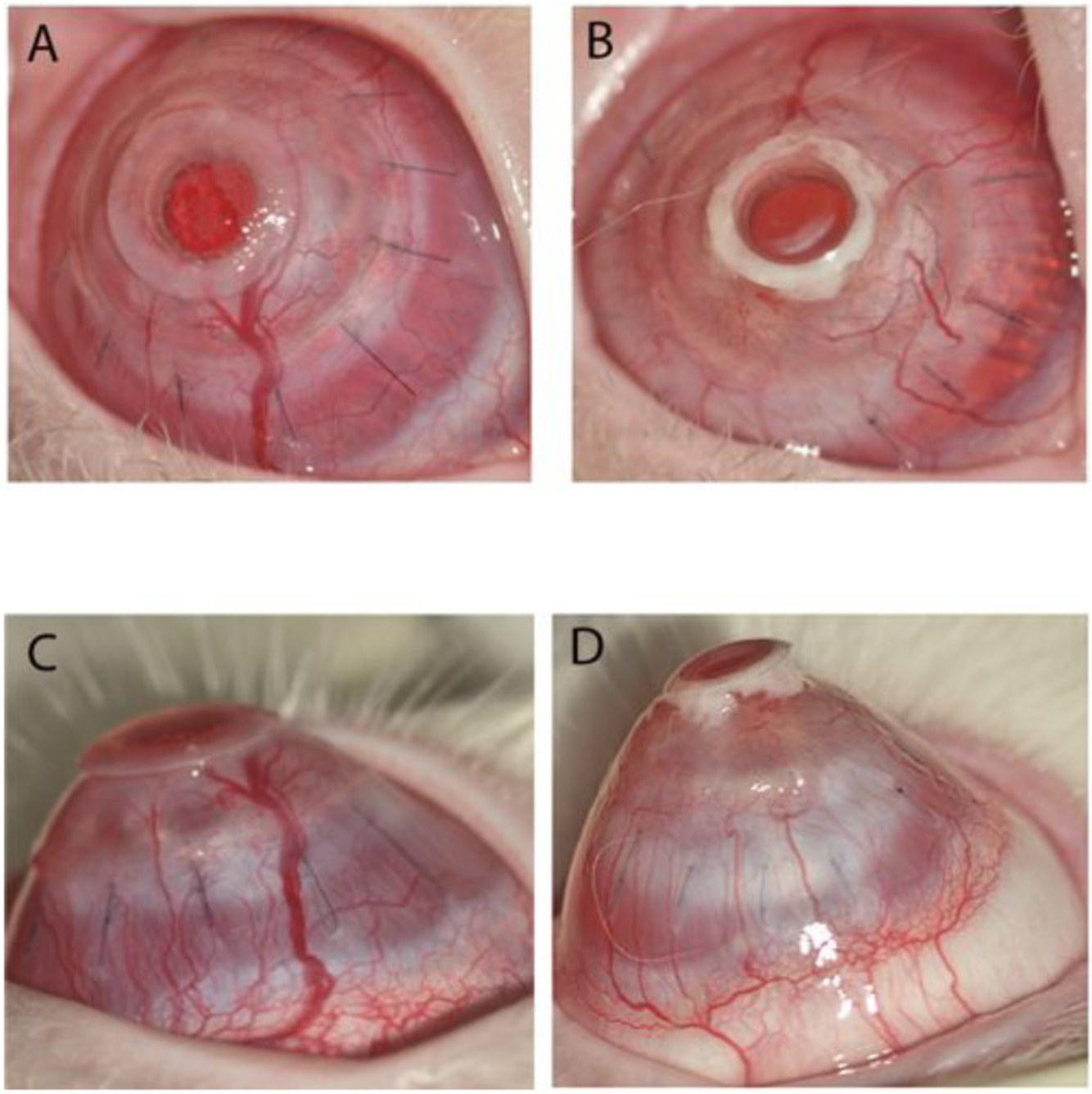


**Figure 7.**

Clinical photographs of an anterior and profile view of comparative B-KPro Type I with a corneal autograft in the New Zealand white rabbit eye at 69 days post-operatively. (**A, C**) In the HMPEI-PMMA B-KPro rabbit eye, there is no mucous accumulation seen behind the front plate, but there is epithelial cell growth over the front plate, moderate neovascularization, and mild conical ectasia. (**B, D**) In the control PMMA B-KPro rabbit eye, there is visible accumulation of cellular debris, mucous in a space behind the front plate, moderate-severe corneal neovascularization, and corneal ectasia.

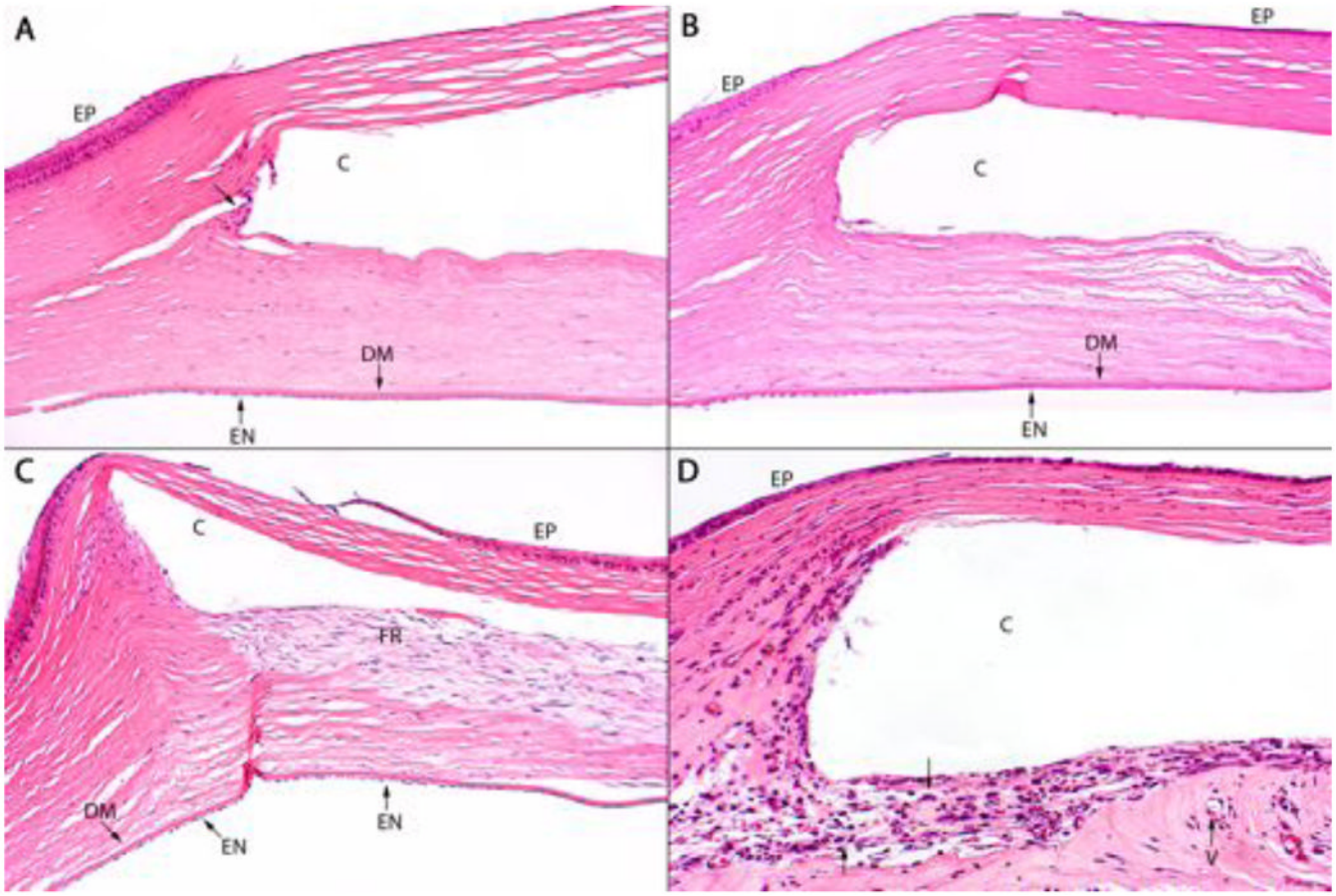


**Figure 8.**

Representative histopathology of a (**A**) HMPEI-Ti disc is shown compared to (**B**) control Ti disc at 61 days post-operatively. There is minimal cellular reactivity at the edges of the disc (arrow) and no significant difference between the two groups (hematoxylin and eosin stain; A ×100, B ×100). Histopathology shown for the HMPEI-PMMA KPro-FP (**C**) compared to control PMMA KPro-FP (**D**), at post-operative day 37. (**C**) HMPEI-PMMA KPro-FP shows minimal inflammatory response and a fibroblastic response is present posterior to the cavity (c) that contained the explanted KPro-FP. (**D**) The uncoated PMMA KPro-FP shows a moderate acute inflammatory response (arrows) surrounding the cavity (c). There is minimal microvascularization (V) (hematoxylin and eosin stain; C ×100, D ×200; DM, Descemet's membrane; EN, endothelium; EP, epithelium).

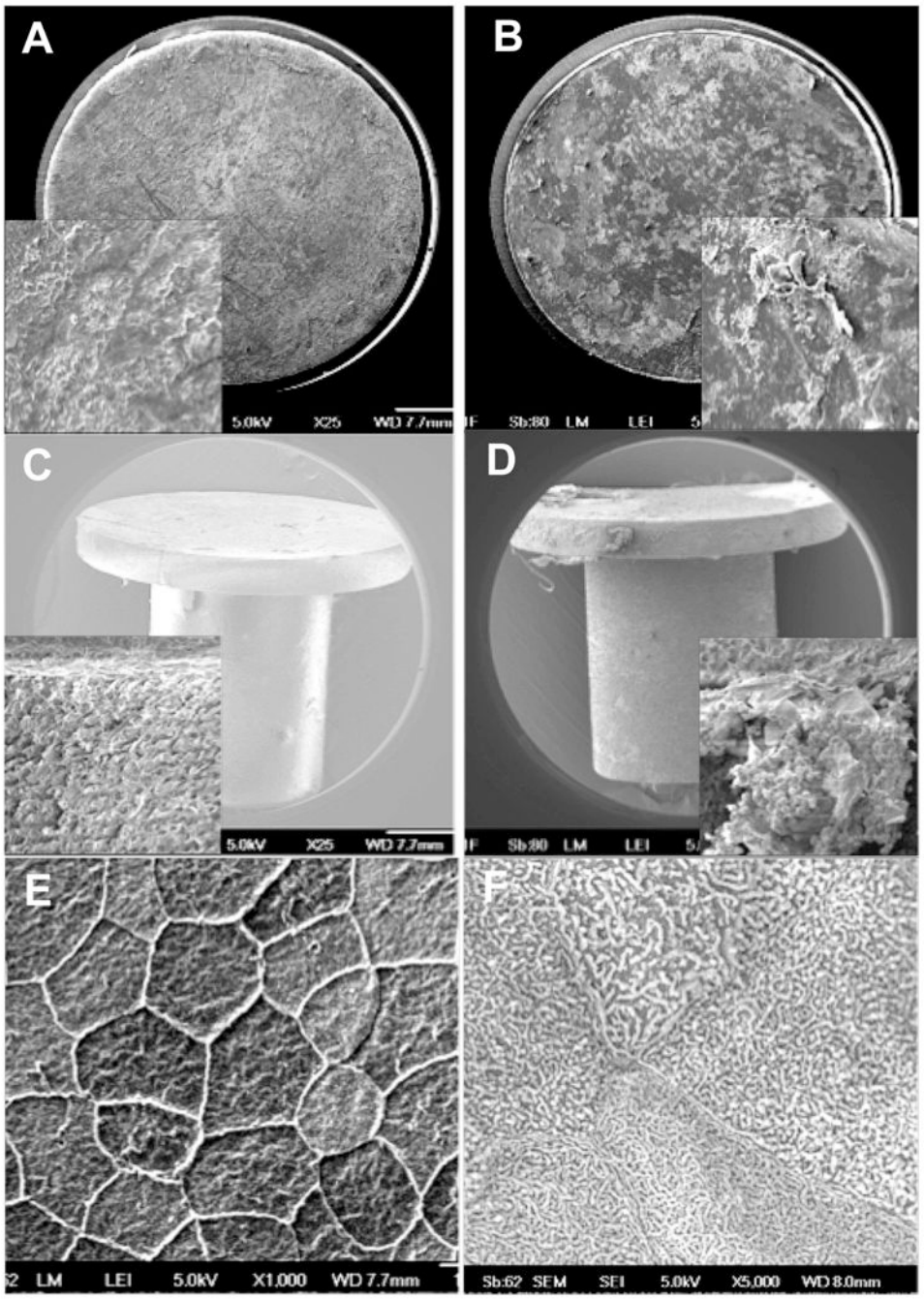


**Figure 9.**

Representative scanning electron micrographs of HMPEI-titanium disc (**A**) compared to a control titanium disc (**B**) extracted from the corneal stroma after 61 days in the rabbit *in vivo*. (**A**) Cells attached to the HMPEI-Ti discs appear smoothly confluent (25X). A higher magnification inset shows a dense “basketweave” of epithelial cells on the HMPEI-Ti disc (500X). (**B**) Cells attached to the control Ti discs demonstrate a less contiguous and more disorganized covering on the uncoated disc (25X). The higher magnification inset shows rolled up edges of discontinuous stromal cells on the control Ti disc (500X). SEMs of (**C**) HMPEI-PMMA KPro-FP compared to (**D**) control PMMA KPro-FP surgically extracted at

post-operative day 105. (**C**) Micrograph shows denser, more compact stromal cells adherent to HMPEI-PMMA KPro-FP (25X). A higher magnification inset shows a dense "basketweave" of epithelial cells (500X). (**D**) There is looser, discontinuous cellular material on the PMMA KPro-FP (25X). The higher magnification inset shows red blood cells in a capillary loosely attached to stromal cells on the front piece (500X). SEMS of (**E**) HMPEI-coated netilicon and (**F**) HMPEI-methafilcon contact lenses at 22 days after placement on the rabbit cornea. (**E**) Micrograph shows organized, smoothly confluent normal mosaic of light, medium, and dark epithelial cells adhering to the HMPEI-coated netilicon contact lens (1000X). (**F**) A higher magnification shows normal epithelial cell microplicae on the HMPEI-coated methafilcon contact lens (5000X).

**Table 1**

Characterization of *Staphylococcus aureus* isolates by clinical source, diagnosis, antibiotic susceptibility pattern, and biofilm formation under different growth conditions using a crystal violet biomass assay. The strongest biofilm clinical isolates are shown at late log growth at 20, 48, and 96 h. A relative biofilm robustness scale (0 – 5) was developed based on 595 nm absorbance readings (Scale: absorbance <0.5 = 0; 0.5 - 0.99 = 1; 1.0 - 1.49 = 2; 1.5 - 1.99 = 3; 2.0 - 2.49 = 4; >2.5 = 5). MSSA, methicillin-sensitive *S. aureus*; MRSA, methicillin-resistant *S. aureus*; Cp-R, ciprofloxacin-resistant; Em-R, erythromycin-resistant; BHI, brain heart infusion; TSB, trypticase soy broth; LB, Luria-Bertoni; suc, sucrose; glc, glucose.

| Strain | Clinical Source | Diagnosis | Antibiotic susceptibility | Biofilm Formation Robustness Scale (0-5) Media and time | | | | |
|---|---|---|---|---|---|---|---|---|
| | | | | BHI 2% suc (h) | TSB 2% glc (h) | LB 1% glc (h) | TSB 0.25% glc (h) | LB 0.1% glc (h) |
| **MEEI-IB001** | **Cornea** (15) | **Keratitis** | **MSSA Cp-R; Em-R** | **5** (24) | | **3** (24) | **1** (24) | **1** (24) |
| | | | | **5** (48) | **1** (48) | **3** (48) | | **1** (48) |
| | | | | **5** (96) | **4** (96) | **2** (96) | | **3** (96) |
| **MEEI-IB002** | **Cornea** | **Keratitis** | **MSSA Cp-R; Em-R** | **5** (24) | | | **1** (24) | **1** (24) |
| **MEEI-IB003** | **Cornea** (15) | **Keratitis** | **MSSA Em-R** | **5** (24) | | **1** (24) | **1** (24) | **1** (24) |
| | | | | **4** (48) | **2** (48) | **4** (48) | | **1** (48) |
| | | | | **5** (96) | **5** (96) | **3** (96) | | **2** (96) |
| **MEEI-IB005** | **Orbit** | **Orbital abscess** | **MSSA** | **5** (24) | | **1** (24) | **1** (24) | **0** (24) |
| | | | | **5** (48) | **2** (48) | **3** (48) | | **0** (48) |
| | | | | **4** (96) | **5** (96) | **2** (96) | | **2** (96) |
| **MEEI-IB011** | **Ear** | **Otitis media** | **MRSA Cp-R; Em-R** | **5** (24) | | **5** (24) | **2** (24) | **0** (24) |
| | | | | **5** (48) | **4** (48) | **5** (48) | | **5** (48) |
| | | | | **5** (96) | **5** (96) | **3** (96) | | **5** (96) |
| **MEEI-IB012** | **Upper lid** (15) | **Eyelid abscess** | **MSSA** | **5** (24) | | | **3** (24) | **1** (24) |
| **MEEI-IB013** | **Canniculus** (15) | **Canniculitis** | **MSSA** | **5** (24) | | | **2** (24) | **0** (24) |
| **MN8** | **Vagina** (19) | **Toxic shock syndrome** | **MSSA** | **2** (24) | | | **1** (24) | |
| | | | | **4** (48) | **3** (48) | **5** (48) | | **0** (48) |
| | | | | **5** (96) | **2** (96) | **2** (96) | | **3** (96) |

| Strain | Clinical Source | Diagnosis | Antibiotic susceptibility | Biofilm Formation Robustness Scale (0-5) Media and time | | | | |
|---|---|---|---|---|---|---|---|---|
| | | | | BHI 2% suc (h) | TSB 2% glc (h) | LB 1% glc (h) | TSB 0.25% glc (h) | LB 0.1% glc (h) |
| **MN8 mucoid** | **Chemostat culture** (18) | **PNAG hyperbiofilm MN8 mutant** | **MSSA** | **4** (24) | | | **4** (24) | |
| | | | | **5** (48) | **5** (48) | **5** (48) | | **5** (48) |
| | | | | **5** (96) | **5** (96) | **5** (96) | | **3** (96) |

**Table 2**

Clinical assessment of the reactivity of HMPEI-coated materials compared to the uncoated parent materials placed in different ocular locations in the New Zealand white rabbit *in vivo*. The number in each group equals n. Graded on a score from 0 (normal) to 4 (severe) with a cumulative score shown in the last row.

| | **Intrastromal PMMA 3-mm disc** | | **Intrastromal titanium 3-mm disc** | | **Intrastromal-anterior chamber KPro-FP** | | **B-KPro-corneal autograft** | |
|---|---|---|---|---|---|---|---|---|
| | **HMPEI-PMMA n = 4** | **PMMA n = 4** | **HMPEI-Ti n = 4** | **Ti n = 4** | **HMPEI-PMMA n = 3** | **PMMA n = 4** | **HMPEI-PMMA n = 1** | **PMMA n = 2** |
| Corneal edema | 0 | 2 | 0 | 0 | 1 | 3 | 1 | 2 |
| Corneal haze/infiltrate | 1 | 3 | 0 | 0 | 1 | 2 | 1 | 3 |
| Corneal neovascularization | 1 | 3 | 0 | 0 | 1 | 4 | 3 | 4 |
| Conjunctival chemosis | 1 | 2 | 1 | 1 | 3 | 3 | 1 | 2 |
| Conjunctival discharge | 0 | 1 | 0 | 0 | 1 | 2 | 1 | 3 |
| Epithelial defects | - | - | - | - | 1 | 4 | - | - |
| Iritis / pupil size | - | - | - | - | 1 / 6 mm | 4 / 10 mm | - | - |
| Anterior chamber flare/cells | - | - | - | - | 1 | 2 | - | - |
| Retroprosthetic membrane | - | - | - | - | 2 | 3 | 1 | 1 |
| Cataract formation | - | - | - | - | 1 | 0 | - | - |
| Total score | 3 | 8 | 1 | 1 | 13 | 27 | 8 | 14 |